Pressure-induced superconductivity in parent CaFeAsF single crystals

Bo Gao,[1] Yonghui Ma,[2,3] Gang Mu,[2,3] and Hong Xiao[1,*]

[1]*Center for High Pressure Science and Technology Advanced Research, Beijing 100094, China*

[2]*State Key Laboratory of Functional Materials for Informatics, Shanghai Institute of Microsystem and Information Technology, Chinese Academy of Sciences, Shanghai 200050, China*

[3]*CAS Center for Excellence in Superconducting Electronics, Shanghai 200050, China*

(Received 15 November 2017; published 4 May 2018)

Flouroarsenide CaFeAsF is a parent compound of the 1111 type of iron-based superconductors. It is similar to the parent LaFeAsO, but it is oxygen-free. To date, studies of pressure-induced effects have only focused on pure and doped polycrystalline CaFeAsF samples. Here, we carried out high-pressure electrical resistivity and Hall coefficient measurements up to 48.2 GPa on single crystals of CaFeAsF. The structural transition temperature T_{str} decreased monotonically upon increasing the pressure, and reached ∼60 K at 9.6 GPa. Superconductivity emerged suddenly at 8.6 GPa with the $T_{c,onset} \sim 25.7$ K, which decreased monotonically with increasing pressure to 5.7 K under 48.2 GPa. Moreover, just after the appearance of superconductivity, the Hall coefficient at 40 K started to decrease with increasing pressure, while keeping its sign negative persisting up to 48.2 GPa.

DOI: 10.1103/PhysRevB.97.174505

I. INTRODUCTION

Until now, high-temperature superconductivity (HTSC) has been achieved in two families: the copper-based oxides (cuprates) and iron-based superconducting materials (FeSCs). Superconductivity (SC) emerges in cuprates and FeSCs through the suppression of the antiferromagnetic (AFM) ordering in their parent materials, which are in a Mott insulating state and a metallic spin-density-wave state, respectively [1,2]. Compared with cuprates, superconductivity in FeSCs can be induced not only by chemical dopants but also by external pressure [3–5]. High-pressure experiments are a powerful tool to investigate the phase diagrams of FeSCs and the mechanism of HTSC.

Pressure as one of the fundamental state parameters can be used to tune the lattice constants and electronic structure efficiently, which thus alter the structural and magnetic ordering. Many high-pressure investigations have been performed on FeSCs, particularly on the 122-type compounds $AEFe_2As_2$ (AE = Ca, Sr, and Ba) [6–14]. Recently, it was found that uniaxial stress seems to strongly suppress the structural phase transition from tetragonal (T) to orthorhombic (O), reduce AFM ordering, and favor the appearance of SC in the T phase in the 122 compounds [7–11]. This clearly indicates that the difference in the hydrostaticity caused by using different pressure media in different pressure cells leads to scattered and confusing results in these early studies. Although the mechanism behind the extreme sensitivity of their properties to uniaxial stress and the origin of filamentary superconductivity are still unclear [7,10], the most intriguing feature of the phase diagram of 122 compounds is that bulk SC competes with the AFM phase [8,9], which is different to that of chemical substitution showing a coexistence of AFM and SC phases [3]. The observed overlap of the SC and AFM phase in the lower-pressure range can be attributed to the coexistence of the O phase and a small amount of the T phase, induced by the inhomogeneity of pressure [8]. For the 1111 family, polycrystalline samples of LaFeAsO and CaFeAsF parents also show SC under pressure as reported in a few works [12–14]. The superconducting transition temperature T_c of LaFeAsO shows a dome-shaped pressure dependency [12]. In contrast, the T_c of CaFeAsF monotonically decreases upon an increase in pressure after the appearance of SC [13,14]. However, since 1111 polycrystalline samples are inhomogeneous in general, and the anomalies in their electrical resistivity curves associated with phase transitions become broad and difficult to distinguish with accuracy at high pressure, the actual phase diagram of the 1111 systems under pressure is presently under debate. More reliable results can be obtained in 1111 single crystals. A recent high-pressure experiment on single-crystal LaFeAsO grown using a NaAs flux shows no bulk superconductivity up to 37 GPa [15,16], which strongly contradicts polycrystalline sample measurements, which show SC under pressure in a wide dome with a maximum T_c of ∼22 K under 12 GPa [12]. This discrepancy may be induced by the difference in the samples grown in their respective synthesis conditions.

Recently, high-quality and reliable single crystals of the undoped parent CaFeAsF were achieved [17,18]. CaFeAsF is another oxygen-free 1111-type parent compound of FeSC, and exhibits high T_c SC induced by 3d transition metals [19,20] and rare-earth elements doping [21], and also applied pressure [13,14]. Furthermore, it is interesting to note that CaFeAsF undergoes a pressure-induced structural phase transition from an orthorhombic (O) to lower symmetry monoclinic (M) structure at low temperature [22], unlike the transition to a high-symmetry phase (O-T) in both the 122 systems [23,24] and LaFeAsO [25] under high pressure. Thus, the high-pressure studies on CaFeAsF would provide an important and deeper

*hong.xiao@hpstar.ac.cn

insight into the correlation between structural modifications and SC under pressure in FeSCs.

In this paper, we report the results of high-pressure electrical resistivity measurements on single crystals of CaFeAsF under pressure up to 48.2 GPa. Compared to polycrystalline samples, our single crystals showed distinct resistive anomalies at the T-O transition temperature T_{str} even to high pressures, providing an opportunity to precisely characterize T_{str} as a function of pressure. The suppression of T_{str} in CaFeAsF is more robust against pressure than the 122 compounds under similar pressure conditions. Pressure-induced SC first emerges at around 8.6 GPa with a $T_{c,onset} \sim 25.7$ K, which decreases monotonically with increasing pressure up to 48.2 GPa. We argue that the SC of CaFeAsF under pressure could be ascribed to the occurrence of an M phase structure.

II. EXPERIMENTAL DETAILS

High-quality single-crystal samples of CaFeAsF were grown using a self-flux method with CaAs as the flux material [17]. Pressure was applied at room temperature using a Be-Cu diamond anvil cell (DAC). Two different pairs of diamond anvils with a culet size of 300 or 500 μm were used in two separate runs to ensure reproducibility. Daphne oil 7373 was used as a pressure-transmitting medium. The BeCu gasket was preindented to 10 GPa in a DAC, and then a hole of 270 μm (for a 300-μm culet) or 460 μm (for a 500-μm culet) in diameter was drilled in the center of the preindented area. The cubic boron nitride (cBN) powders were added inside the indent, which were then pressed to 15 GPa (for a 500-μm culet) or 25 GPa (for a 300-μm culet) again, reliably insulating the sample and electrodes against the BeCu metallic gasket. Finally a hole of 200 μm (for a 500-μm culet) or 140 μm (for a 300-μm culet) in diameter was drilled in the center of the cBN gasket again. Four hand-cut platinum (Pt) thin wires were attached to the samples with sliver epoxy. A CaFeAsF single crystal was cut into dimensions of about $100 \times 100 \times 20$ or $75 \times 75 \times 20\,\mu$m for 500- and 300-$\mu$m culets, respectively. The pressure was determined using the ruby fluorescence shift at room temperature. The van der Pauw method was used to complete high-pressure electrical resistivity and Hall coefficient measurements on the CaFeAsF crystals, with the electrical current along the ab plane and the magnetic field along the c axis. The Hall coefficient was measured by sweeping the magnetic field from -9 to 9 T at 40 K.

III. RESULTS AND DISCUSSION

Figure 1 shows the temperature-dependent electrical resistivity $\rho(T)$ of a CaFeAsF single crystal under pressures up to 48.2 GPa, obtained with a culet size of 300 μm in run 1. At ambient pressure, the $\rho(T)$ of CaFeAsF shows a remarkable drop at $\sim$118 K during cooling [18], which is much sharper than the polycrystalline samples. This anomaly in the resistivity corresponds to the T-O structural transition, in reasonable agreement with the previously reported powder synchrotron x-ray measurements of a $T_{str} \sim 120$ K [26,27].

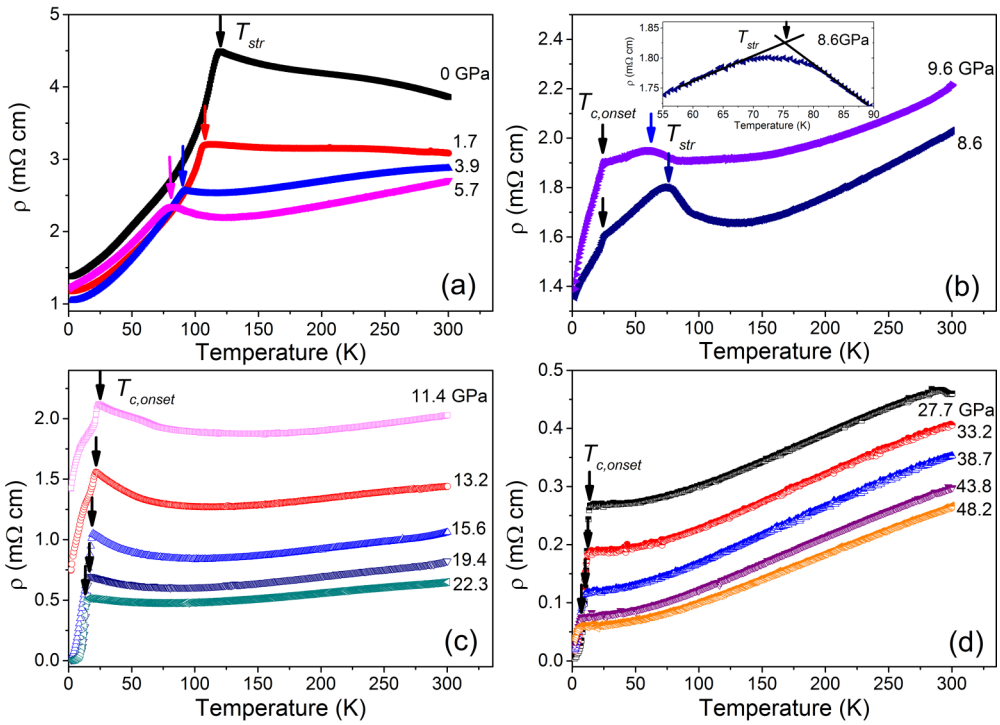

FIG. 1. Temperature-dependent electrical resistivity $\rho(T)$ of CaFeAsF single crystal under pressures (run 1) up to 48.2 GPa. The vertical arrows at the T_{str} and $T_{c,onset}$ indicate the T-O structural transition temperature and the onset temperature of the superconducting transition, respectively. The inset of (b) shows the expanded view of $\rho(T)$ near the structural transition and method of determining the value of the T_{str} at 8.6 GPa.

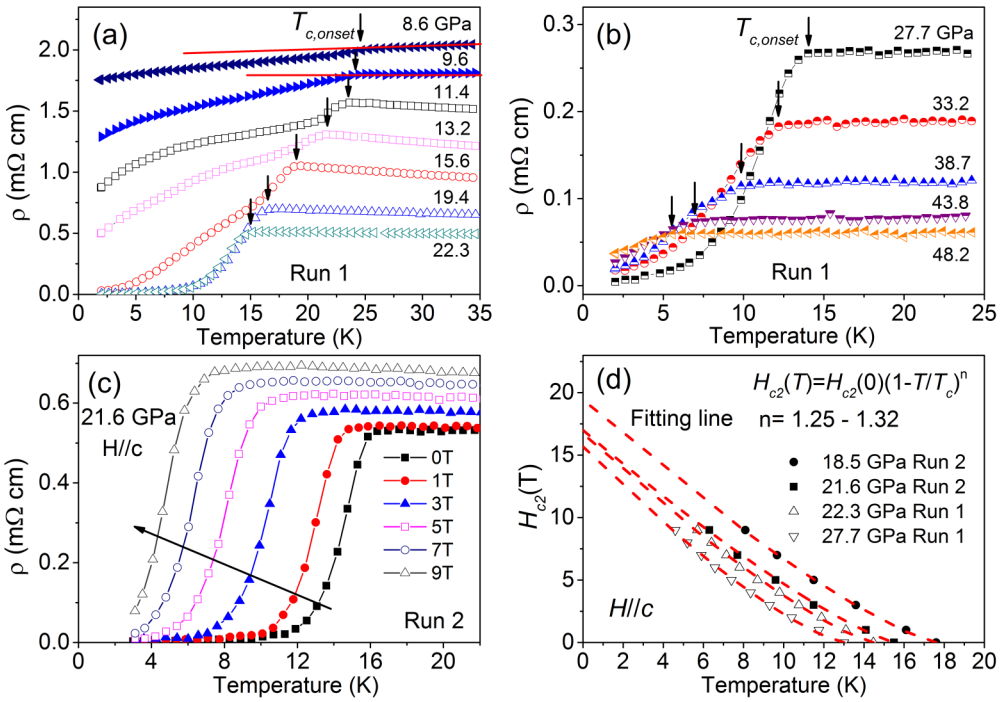

FIG. 2. (a, b) Expanded view of $\rho(T)$ of CaFeAsF above 5.7 GPa at low temperature. The $T_{c,\mathrm{onset}}$ is indicated by arrows (run 1). Some curves in (a) have been offset for clarity. (c) Temperature dependence of the CaFeAsF resistance under different fields up to 9 T at 21.6 GPa (run 2). (d) Temperature dependence of the CaFeAsF upper critical field (H_{c2}) under pressure.

With increasing pressure, the anomaly at T_{str} shifts downwards to lower temperature and remains clearly visible up to 9.6 GPa. So, T_{str} is defined by the intersection of two extrapolated lines drawn through the resistivity curve below and above the anomaly, as shown in the inset of Fig. 1(b). T_{str}, as marked by the arrows in Figs. 1(a) and 1(b), decreases with a slope of $dT_{\mathrm{str}}/dP = -6.25\,\mathrm{K/GPa}$ and seems to disappear above 9.6 GPa. Under similar pressure conditions, the collapse of T-O transition of $BaFe_2As_2$ occurs around 3–4 GPa, using DAC and Daphne oil 7373 or 7474 as pressure transmitting medium [7,8]. It seems that the suppression of the CaFeAsF T-O transition is more robust against pressure than the 122 compounds. Meanwhile, at 8.6 and 9.6 GPa, we observe a sizeable reduction of resistivity below ~25.7 K that is strongly suppressed by applying magnetic fields, suggesting a SC transition. Upon further pressure increase, this resistivity drop becomes larger and steeper, and finally zero resistivity was detected above 19.4 GPa, where a pressure-induced SC was indeed further confirmed. An expanded view of the $\rho(T)$ above 8.6 GPa at low temperatures is shown in Figs. 2(a) and 2(b). Here we define the onset temperature of the superconducting transition, $T_{c,\mathrm{onset}}$, by the deviation from the linearity of normal-state resistivity $\rho(T)$ above the T_c, as indicated by arrows in Figs. 1, 2(a), and 2(b). The $T_{c,\mathrm{onset}}$ decreases monotonically against pressure, although SC persists up to the highest studied pressure of 48.2 GPa. Above 27.7 GPa, the SC transition tends to broaden again without the zero-resistivity state. The absence of zero resistivity at lower pressure may be due to the small superconducting fraction of the sample below the percolation limit, as we discuss below. The disappearance of zero resistivity under high pressure above 27.7 GPa could be related to the presence of microcracks due to the serious nonhydrostatic conditions [28]. Interestingly, the $\rho(T)$ shows an upturn behavior before the T_{str} or $T_{c,\mathrm{onset}}$, which becomes less distinct upon increasing pressure and finally disappears above 27.7 GPa. A similar phenomenon as a function of the doping level is also observed in the Co- and Ni-doped CaFeAsF compounds [20,29]. The origin of this upturn behavior in the resistivity trace is still unclear [30]. But our high-pressure results can rule out the simple scenario of the scattering center increase induced by the replacement of Fe with Co or Ni in FeAs superconducting layers [13].

We repeated the high-pressure $\rho(T)$ measurement on another CaFeAsF single crystal with a culet size of 500 μm (run 2). Similar superconducting behavior with almost identical T_c was observed under pressures up to 21.6 GPa. The $\rho(T)$ curves for the magnetic field up to 9 T at 21.6 GPa (run 2) are shown in Fig. 2(c). There is a monotonic suppression of the superconducting transition, with modest broadening in the fields. Figure 2(d) shows that if the upper critical fields $H_{c2}(T)$ of CaFeAsF under 18.5–27.7 GPa for the $H//c$ axis were determined by adopting different criteria 90% of $\rho(T_{c,\mathrm{onset}})$, there is a clear upward curvature in $H_{c2}(T)$, which cannot be explained by the one-gap Werthamer-Helfand-Hohenberg theory. This feature indicates the multiband nature of SC in CaFeAsF under pressure. The experimental $H_{c2}(T)$ data can be described within the entire T/T_c range by the expression $H_{c2}(T) = H_{c2}(0)(1\text{-}T/T_c)^{\mathrm{n}}$ [31,32], giving a $H_{c2}(0) \sim$ 15–20 T of CaFeAsF in the pressure range of 18.5–27.7 GPa.

Figures 3(a) and 3(b) show the Hall resistivity $\rho_{xy}(H)$ of the CaFeAsF single crystals at 40 K under various pressures. The $\rho_{xy}(H)$ at 3.9 and 5.7 GPa share similar features with

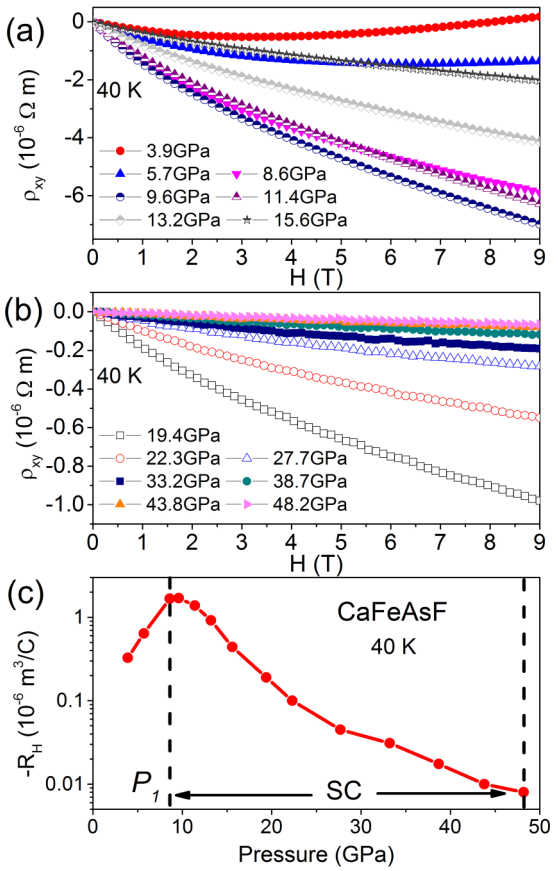

FIG. 3. (a, b) Field dependence of Hall resistivity $\rho_{xy}(H)$ of the CaFeAsF single crystal at 40 K at pressures up to 48.2 GPa. (c) Pressure dependence of the Hall coefficient R_H of CaFeAsF at 40 K.

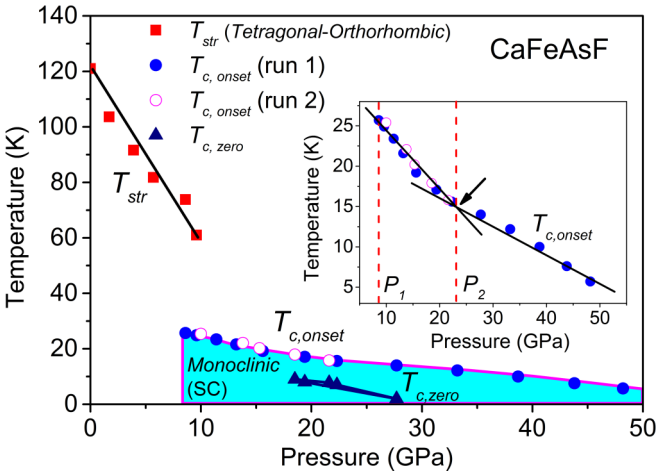

FIG. 4. The pressure-temperature diagram of CaFeAsF obtained by electrical resistivity measurements. The onset of T_c, $T_{c,\mathrm{onset}}$, is defined by the deviation from the linearity of normal-state resistivity $\rho(T)$ above T_c, and $T_{c,\mathrm{zero}}$ is defined by temperature at which ρ becomes zero. The inset shows the $T_{c,\mathrm{onset}}$ dependence under pressure.

those at ambient pressure. A nonlinearity develops for $\rho_{xy}(H)$ and the slope changes sign from negative to positive with the increase of magnetic field. Upon increasing pressure to above 8.6 GPa, all $\rho_{xy}(H)$ curves exhibit a negative slope in the whole investigated magnetic-field range, but nonlinearity also appears. Figure 3(c) shows the pressure dependence of the Hall coefficient, defined as the field derivative of $\rho_{xy}(H)$, $R_H \equiv d\rho_{xy}(H)/dH$, in a zero-field limit. The sign of R_H is clearly negative in the whole pressure range, suggesting electrons are the dominant charge carriers. Notably at ambient pressure, the R_H in our CaFeAsF single crystal is measured and shown to be negative below T_{str}, which confirms that the negative R_H is an intrinsic property of CaFeAsF and resolves the discrepancy in the sign of R_H below the T_{str} in CaFeAsF polycrystalline samples where both negative and positive R_H were previously reported [21,29]. It is also the same as the other oxygen-derivative 1111 and 122 parents, showing the electron characteristics of its dominative carriers. As shown in Fig. 3(c), the amplitude of R_H increases initially with pressure, but once the pressure is increased above a critical value $P_1 = 8.6$ GPa where SC starts to appear it starts to decrease, producing a peak-shaped dependence of R_H with pressure. Such a significant change in the pressure dependence of R_H reflects a pronounced change in the band structure of CaFeAsF under pressure, which might be explained by the appearance of the O-M structural transition as we discuss below. The emergence of superconductivity and the change of the R_H-pressure dependence at the same pressure indicate a close connection between them. In addition, in the SC phase, both the R_H and T_c decrease against pressure, showing similar pressure dependence behavior.

In Fig. 4 we have constructed a phase diagram for CaFeAsF under pressures. It is shown that T_{str} decreases linearly with increasing pressures, reaching ~60 K at 9.6 GPa. Pressure-induced SC starts to appear under $P_1 \sim 8.6$ GPa at 25.7 K, and the $T_{c,\mathrm{onset}}$ decreases monotonically with increasing pressure. As shown in the inset of Fig. 4, the pressure dependence of the $T_{c,\mathrm{onset}}$ also exhibits a kink around a critical pressure of $P_2 \sim 23.0$ GPa. The $T_{c,\mathrm{onset}}$ varies linearly on either side of P_2, but with different slopes. Note that this pressure P_2 is near the position where the upturn behavior in resistivity disappears before the $T_{c,\mathrm{onset}}$. Okada *et al.* used two different cells and pressure transmitting media, a cubic anvil cell with Daphne 7474 liquid and a DAC with NaCl powder, respectively [13]. They found the $T_{c,\mathrm{onset}}$ of 29 K appears under similar pressures of 4–5 GPa, which is consistent with that obtained in a DAC with steatite by Freitas *et al.* [14]. The observed P_1 and $T_{c,\mathrm{onset}}$ in our paper are slightly higher and lower than those obtained in polycrystalline samples by Okada *et al.* [13] and Freitas *et al.* [14], respectively.

On the other hand, we note that the resistivity drop becomes larger upon increasing pressure from 8.6 to 15.6 GPa. The pressure interval is too large to be explained simply by the sample pressure gradients within the Daphne 7373 liquid inside the DAC. And, it should be mentioned that this feature is accompanied by the decrease of the onset T_c during this pressure regime. One of the most possible explanations for these above features is that two phases coexist and the percentage of SC phases in the crystals continuously increases with pressure. Mishra *et al.* reported that CaFeAsF undergoes an O-M phase transition at 13.7 GPa, and this new M phase remains stable up to 40 GPa at 40 K [22]. Consequently, we speculate that the M phase is superconducting in CaFeAsF. The inconsistency

between the O-M transition pressure point reported by Mishra *et al.* and P_1 for SC appearance, as well as the change of the transition to structural phase mixtures obtained in our case, may be due to the different thermodynamic history (pressure and temperature). In our case, high-pressure $R(T)$ measurements were performed upon cooling from room temperature at fixed values of pressures, with a liquid pressure transmitting medium Daphne oil 7373, which solidifies above 2.2 GPa at room temperature. Mishra *et al.* used helium as a pressure medium to provide the best hydrostatic conditions; the sample was first cooled from 300 to 100 K below 2 GPa, cooled to 40 K below 5.8 GPa, and then pressurized to 40 GPa at a fixed temperature of 40 K. The difference in the compression conditions of the samples may cause different phase-transition behaviors, which has already been observed in the 122 systems under pressure [23]. Moreover, the less hydrostatic pressure gradient in our case might considerably suppress the O-M phase transition pressure lower than 13.7 GPa and also cause the coexistence of these two phases at low temperature in CaFeAsF. Further, the SC of CaFeAsF is quite robust under high pressure up to 48.2 GPa. In contrast, in the 122 systems, SC occurs in a much narrower pressure range in the T phase. In this experiment, unfortunately, the exact pressure range for the coexistence of O and M phases is difficult to identify.

IV. CONCLUSIONS

We measured the electrical resistivity and Hall coefficient of single-crystalline samples of CaFeAsF under applied pressure up to 48.2 GPa to determine the phase diagram. We found that the T-O structural transition temperature is suppressed upon increasing pressure. Superconductivity starts to appear around 8.6 GPa, and the $T_{c,\mathrm{onset}}$ decreases monotonically with increasing pressure, reaching 5.7 K at 48.2 GPa. Moreover, electronlike charge carriers are dominant during the whole pressure range. After the appearance of the SC phase, the Hall coefficient at 40 K decreases against pressure, indicating an enhancement in the charge carriers. By comparing our results with previous x-ray-diffraction measurements under pressure [22], we argued that SC can coexist with the low-temperature monoclinic phase. The overlap of the T-O transition and SC phase might be caused by the nonhydrostaticity of the pressure or uniaxial stress.

ACKNOWLEDGMENTS

The work is supported by National Science Associated Funding (No. U153042), the "Strategic Priority Program (B)" of the Chinese Academy of Sciences (No. XDB04040300), and the Youth Innovation Promotion Association of the Chinese Academy of Sciences (No. 2015187).

[1] A. S. Sefat, Rep. Prog. Phys. **74**, 124502 (2011).
[2] X. H. Chen, P. C. Dai, D. L. Feng, T. Xiang, and F. C. Zhang, Natl. Sci. Rev. **1**, 371 (2014).
[3] G. R. Stewart, Rev. Mod. Phys. **83**, 1589 (2011).
[4] J. Paglione and R. L. Greene, Nat. Phys. **6**, 645 (2010).
[5] M. S. Torikachvili, S. L. Bud'ko, N. Ni, and P. C. Canfield, Phys. Rev. Lett. **101**, 057006 (2008).
[6] S. Medvedev, T. M. McQueen, I. A. Troyan, T. Palasyuk, M. I. Eremets, R. J. Cava, S. Naghavi, F. Casper, V. Ksenofontov, G. Wortmann, and C. Felser, Nat. Mater. **8**, 630 (2009).
[7] W. J. Duncan, O. P. Welzel, C. Harrison, X. F. Wang, X. H. Chen, F. M. Grosche, and P. G. Niklowitz, J. Phys.: Condens. Matter **22**, 052201 (2010).
[8] T. Yamazaki, N. Takeshita, R. Kobayashi, H. Fukazawa, Y. Kohori, K. Kihou, C.-H. Lee, H. Kito, A. Iyo, and H. Eisaki, Phys. Rev. B **81**, 224511 (2010).
[9] K. Matsubayashi, N. Katayama, K. Ohgushi, A. Yamada, K. Munakata, T. Matsumoto, and Y. Uwatoko, J. Phys. Soc. Jpn. **78**, 073706 (2009).
[10] W. Yu, A. A. Aczel, T. J. Williams, S. L. Bud'ko, N. Ni, P. C. Canfield, and G. M. Luke, Phys. Rev. B **79**, 020511(R) (2009).
[11] K. Prokeš, A. Kreyssig, B. Ouladdiaf, D. K. Pratt, N. Ni, S. L. Bud'ko, P. C. Canfield, R. J. McQueeney, D. N. Argyriou, and A. I. Goldman, Phys. Rev. B **81**, 180506(R) (2010).
[12] H. Okada, K. Igawa, H. Takahashi, Y. Kamihara, M. Hirano, H. Hosono, K. Matsubayashi, and Y. Uwatoko, J. Phys. Soc. Jpn. **77**, 113712 (2008).
[13] H. Okada, H. Takahashi, S. Matsuishi, M. Hirano, H. Hosono, K. Matsubayashi, Y. Uwatoko, and H. Takahashi, Phys. Rev. B **81**, 054507 (2010).
[14] D. C. Freitas, G. Garbarino, R. Weht, A. Sow, X. Zhu, F. Han, P. Cheng, J. Ju, H. H. Wen, and M. Núñez-Regueiro, J. Phys.: Condens. Matter **26**, 155702 (2014).
[15] A. Jesche, F. Nitsche, S. Probst, T. Doert, P. Müller, and M. Ruck, Phys. Rev. B **86**, 134511 (2012).
[16] C. A. McElroy, J. J. Hamlin, B. D. White, S. T. Weir, Y. K. Vohra, and M. B. Maple, Phys. Rev. B **90**, 125134 (2014).
[17] Y. Ma, H. Zhang, B. Gao, K. Hu, Q. Ji, G. Mu, F. Huang, and X. Xie, Supercond. Sci. Technol. **28**, 085008 (2015).
[18] T. Terashima, H. T. Hirose, D. Graf, Y. Ma, G. Mu, T. Hu, K. Suzuki, S. Uji, and H. Ikeda, Phys. Rev. X **8**, 011014 (2018).
[19] S. Matsuishi, Y. Inoue, T. Nomura, H. Yanagi, M. Hirano, and H. Hosono, J. Am. Chem. Soc. **130**, 14428 (2008).
[20] S. Matsuishi, Y. Inoue, T. Nomura, Y. Kamihara, M. Hirano, and H. Hosono, New J. Phys. **11**, 025012 (2009).
[21] P. Cheng, B. Shen, G. Mu, X. Zhu, F. Han, B. Zeng, and H.-H. Wen, Europhys Lett. **85**, 67003 (2009).
[22] S. K. Mishra, R. Mittal, S. L. Chaplot, S. V. Ovsyannikov, D. M. Trots, L. Dubrovinsky, Y. Su, Th. Brueckel, S. Matsuishi, H. Hosono, and G. Garbarino, Phys. Rev. B **84**, 224513 (2011).
[23] R. Mittal, S. K. Mishra, S. L. Chaplot, S. V. Ovsyannikov, E. Greenberg, D. M. Trots, L. Dubrovinsky, Y. Su, Th. Brueckel, S. Matsuishi, H. Hosono, and G. Garbarino, Phys. Rev. B **83**, 054503 (2011).
[24] A. I. Goldman, A. Kreyssig, K. Prokeš, D. K. Pratt, D. N. Argyriou, J. W. Lynn, S. Nandi, S. A. J. Kimber, Y. Chen, Y. B. Lee, G. Samolyuk, J. B. Leão, S. J. Poulton, S. L. Bud'ko, N. Ni, P. C. Canfield, B. N. Harmon, and R. J. McQueeney, Phys. Rev. B **79**, 024513 (2009).
[25] R. S. Kumar, J. J. Hamlin, M. B. Maple, Y. Zhang, C. Chen, J. Baker, A. L. Cornelius, Y. Zhao, Y. Xiao, S. Sinogeikin, and P. Chow, Appl. Phys. Lett. **105**, 251902 (2014).
[26] Y. Xiao, Y. Su, R. Mittal, T. Chatterji, T. Hansen, C. M. N. Kumar, S. Matsuishi, H. Hosono, and Th. Brueckel, Phys. Rev. B **79**, 060504(R) (2009).

[27] T. Nomura, Y. Inoue, S. Matsuishi, M. Hirano, J. E. Kim, K. Kato, M. Takata, and H. Hosono, Supercond. Sci. Technol. **22**, 055016 (2009).

[28] E. Colombier, M. S. Torikachvili, N. Ni, A. Thaler, S. L. Bud'ko, and P. C. Canfield, Supercond. Sci. Technol. **23**, 054003 (2010).

[29] M. Zhang, C. Zhang, Y. Yu, L. Zhang, Z. Qu, L. Ling, C. Xi, S. Tan, and Y. Zhang, New J. Phys. **12**, 083050 (2010).

[30] D. Bérardan, L. Zhao, L. Pinsard-Gaudart, and N. Dragoe, Phys. Rev. B **81**, 094506 (2010).

[31] K.-H. Müller, G. Fuchs, A. Handstein, K. Nenkov, V. N. Narozhnyi, and D. Eckert, J. Alloys and Compd. **322**, L10 (2001).

[32] X.-C. Pan, X. Chen, H. Liu, Y. Feng, Z. Wei, Y. Zhou, Z. Chi, L. Pi, F. Yen, F. Song, X. Wan, Z. Yang, B. Wang, G. Wang, and Y. Zhang, Nat. Commun. **6**, 7805 (2015).